Journal of Modern Optics
Vol. 57, No. 3, 10 February 2010, 198–206

Taylor & Francis
Taylor & Francis Group

The discrimination problem for two ground states or two thermal states of the quantum Ising model

Carmen Invernizzi[a] and Matteo G.A. Paris[a,b,c*]

[a]*Dipartimento di Fisica, Università degli Studi di Milano, Italy;* [b]*CNISM UdR Milano, I-20133 Milano, Italy;* [c]*ISI Foundation, I-10133 Torino, Italy*

(*Received 6 May 2009; final version received 22 July 2009*)

We address the one-dimensional quantum Ising model as an example of a system exhibiting criticality and study in some details the discrimination problem for pairs of states corresponding to different values of the coupling constant. We evaluate the error probability for single-copy discrimination, the Chernoff bound for n-copy discrimination in the asymptotic limit, and the Chernoff metric for the discrimination of infinitesimally close states. We point out scaling properties of the above quantities, and derive the external field optimizing state discrimination for short chains as well as in the thermodynamical limit, thus assessing criticality as a resource for quantum discrimination in many-body systems.

Keywords: state discrimination; Ising model; distance between quantum states; Chernoff bound

1. Introduction

In quantum state discrimination one should determine the state of a quantum system based on the outcome of a certain measurement, and assuming that the system may be prepared in a state chosen from a given list of possible candidates. Of course, when the candidate states are not orthogonal, basic quantum mechanics dictates that no measurement can distinguish perfectly between them. The objective is therefore to choose some figure of merit characterizing the quality of the state discrimination and optimize it over the space of allowed quantum measurements. This procedure, known as quantum state discrimination or quantum hypothesis testing [1–4], plays a relevant role in the characterization of signals and devices and, in turn, in the development of quantum technology.

The two main paradigms of state discrimination are unambiguous identification [5–9] and (ambiguous) minimum error discrimination [10–15]. In the first method, to discriminate among N states one searches a measurement with $N+1$ outcomes, where the additional result accounts for inconclusive detection, and in turn allows the conclusive determination in the remaining cases. On the other hand, in ambiguous discrimination one looks for a measurement with N outcomes, always leading to a determination of the state, while accepting the possibility of a wrong inference. In this paper we restrict ourselves to the second method, which basically consists in looking for the optimal measurement that minimizes the probability of errors, i.e. the overall probability of a misidentification. For the discrimination between two states, pure or mixed, the optimal measurement and the minimum error probability had been derived by Helstrom [1]. If n copies of the system are available the scaling of the error probability with the number of copies may be expressed using the so-called quantum Chernoff bound ξ_{QCB} [16,17]. In particular, it has been proved that ξ_{QCB} defines a meaningful distinguishability measure when one has to solve the problem of discriminating two sources that output many identical copies of two quantum states. In addition, when considering two states that are infinitesimally close, the quantum Chernoff bound induces a metric on the manifold of quantum states.

In this paper we study the discrimination problem for two ground states or two thermal states of the Ising model in a transverse magnetic field, which represents a paradigmatic example of a system which undergoes a second-order quantum phase transition (QPT). We consider the system both at zero and finite temperature, and address discrimination of states corresponding to different values of the coupling parameter. In particular, we evaluate the error probability for single-copy discrimination, the Chernoff bound for n-copy discrimination in the asymptotic limit, and the Chernoff metric for the discrimination of infinitesimally close states. We are interested in the

*Corresponding author. Email: matteo.paris@unimi.it

ISSN 0950–0340 print/ISSN 1362–3044 online

DOI: 10.1080/09500340903205173
http://www.informaworld.com

scaling properties of the above quantities with the coupling itself, the temperature and the size of the system. Moreover, we look for the optimal value of the field that minimizes the probability of error and maximizes both the Chernoff bound and the corresponding metric. It turns out that criticality is a resource for quantum discrimination of states. Indeed, at zero temperature the critical point signs a minimum in the probability of error and a divergence in the QCB metric. Remarkably, despite the fact that the Chernoff metric is associated with quantum discrimination and the Bures metric is related to quantum estimation [18,19], these different measures show the same critical behavior and carry the same information about the QPT of the system [20].

The paper is organized as follows. In Section 2 we introduce the model. In Section 3 we review the basic elements of quantum state discrimination and also illustrate the notion of the quantum Chernoff metric for the Ising model. In Section 4 we study the distinguishability of states at zero temperature, both for the case of a few spins and then in the thermodynamic limit. In Section 5 we consider the effects of temperature and the scaling properties of the metric. Section 6 closes the paper with some concluding remarks.

2. Quantum Ising model

We consider the one-dimensional Ising model of size L as an example of a system which undergoes a zero-temperature quantum phase transition [21–23]. The model is defined by the Hamiltonian

$$H = -J\sum_{k=1}^{L}\sigma_k^x\sigma_{k+1}^x - h\sum_{k=1}^{L}\sigma_k^z, \tag{1}$$

where the σ_k^α are Pauli operators for the kth site. We also assume periodic boundary conditions $\sigma_{L+1}^x = \sigma_1^x$. As the temperature and the field h are varied one may identify different physical regions. At zero temperature, the system undergoes a QPT for $h = J$ and becomes gapless. For $h < J$ the system is in an ordered phase whereas for $h > J$ the field dominates, and the system is in a paramagnetic state. For temperature $T \ll \Delta$, $\Delta = |J - h|$ the system behaves quasi-classically, whereas for $T \gg \Delta$ quantum effects dominate. The Hamiltonian (1) can be exactly diagonalized by a Bogoliubov transformation, leading to

$$H = \sum_{k>0}\Lambda_k\left(\eta_k^\dagger\eta_k - 1\right), \tag{2}$$

where Λ_k denotes the one particle energies and η_k the annihilation operator, $\Lambda_k = (\epsilon_k^2 + \Delta_k^2)^{1/2}$, $\Delta_k = J\sin(k)$, $\varepsilon_k = (J\cos(k) + h)$. The one-particle excitations are created by the action of $\eta_k^\dagger = \cos(\theta_k/2)d_k^\dagger + \mathrm{i}\sin(\theta_k/2)d_{-k}$ on the ground state

$$|\psi_0\rangle = \bigotimes_k\left[\cos\left(\frac{\theta_k}{2}\right)|00\rangle_{k,-k} + \mathrm{i}\sin\left(\frac{\theta_k}{2}\right)|11\rangle_{k,-k}\right], \tag{3}$$

where $\vartheta_k = \tan^{-1}(\epsilon_k/\Delta_k)$ and $d_k|00\rangle_{k,-k} = d_{-k}|00\rangle_{-k,k} = \eta_k|\psi_0\rangle = 0$. Strictly speaking, Equation (2) holds in the sector with even number of fermions. In this case, periodic boundary conditions on the spins induce antiperiodic BCs on the fermions and the momenta satisfy $k = [(2n+1)\pi]/L$. In the sector with odd number of particles, instead, one has $k = [(2n)\pi]/L$ and one must carefully treat excitations at $k = 0$ and $k = \pi$. In any case, the ground state of (1) belongs to the even sector so that, at zero temperature we can use Equation (2) for any finite L. At positive temperature we will be primarily interested in large system sizes and therefore we can neglect boundary terms in the Hamiltonian and use Equation (2) in the whole Fock space.

3. Elements of quantum states discrimination

Suppose we have a quantum system which may be prepared in different states ρ_k, $k = 1, \ldots, N$, chosen from a given set, with *a priori* probability z_k, $\sum_k z_k = 1$. A discrimination problem arises in any situation where the system is presented to an experimenter who has to infer the state of system by performing a measurement. The states are known, as well as the *a priori* probabilities, but we don't know which state has been actually sent to the observer. The simplest case occurs when the system may be prepared in two possible states, described by the density matrices ρ_1 and ρ_2, with *a priori* probabilities z_1 and $z_2 = 1 - z_1$. Any strategy for the (ambiguous) discrimination between these two states amounts to defining a two-outcomes POVM $\{E_1, E_2\}$ on the system, where $E_1 + E_2 = \mathbb{I}$ and $E_k \geq 0\ \forall k$. After observing the outcome j the observer infers that the state of the system is ρ_j. The probability of inferring the state ρ_j when the true state is ρ_k is thus given by $P_{jk} = \mathrm{Tr}[\rho_k E_j]$ and the optimal POVM for the discrimination problem is the one minimizing the overall probability of a misidentification, i.e. $P_\mathrm{e} = z_1 P_{21} + z_2 P_{12}$. For the simplest case of equiprobable hypotheses ($z_1 = z_2 = 1/2$) we have $P_\mathrm{e} = \frac{1}{2}(1 - \mathrm{Tr}[E_2\Gamma])$, where $\Gamma = \rho_2 - \rho_1$. P_e is minimized by choosing E_2 as the projector over the positive subspace of Γ. Then we have $\mathrm{Tr}[E_2\Gamma] = \mathrm{Tr}|\Gamma|$ and $P_\mathrm{e} = \frac{1}{2}(1 - \mathrm{Tr}|\Gamma|)$, where $|A| = (A^\dagger A)^{1/2}$.

When $\rho_k = |\psi_k\rangle\langle\psi_k|$ are pure states the error probability reduces to $P_e = \frac{1}{2}(1 - (1 - |\langle\psi_1|\psi_2\rangle|^2)^{1/2}|)$.

Let us now suppose that n copies of both ρ_1 and ρ_2 are available for the discrimination. The problem may be addressed using the above formulas upon replacing ρ with $\rho^{\otimes n}$. We thus need to analyze the quantity $P_{e,n} = \frac{1}{2}(1 - \mathrm{Tr}|\rho_2^{\otimes n} - \rho_1^{\otimes n}|)$. It turns out that in the asymptotic limit of large n the error probability decreases exponentially with n as $P_{e,n} \sim \exp(-n\xi_{\mathrm{QCB}})$, where the quantity ξ_{QCB} is called the *quantum Chernoff bound* (QCB) and may be evaluated as follows [16]

$$\xi_{\mathrm{QCB}} = -\log \min_{0\le s\le 1} \mathrm{Tr}\left[\rho_1^s \rho_2^{1-s}\right]. \tag{4}$$

For pure states QCB achieves its superior limit, which is given in terms of the overlap between the two states $\xi_{\mathrm{QCB}} = -\log|\langle\psi_1|\psi_2\rangle|^2$. The QCB introduces a measure of distinguishability for density operators which acquires an operational meaning in the asymptotic limit. For a fixed probability of error P_e, the larger is the ξ_{QCB}, the smaller the number of copies of ρ_1 and ρ_2 we will need in order to distinguish them.

Upon considering two nearby states ρ and $\rho + \mathrm{d}\rho$, the QCB induces the following distance over the manifold of quantum states

$$\mathrm{d}s^2_{\mathrm{QCB}} := 1 - \exp(-\xi_{\mathrm{QCB}}) = \frac{1}{2}\sum_{m,n} \frac{|\langle\varphi_m|\mathrm{d}\rho|\varphi_n\rangle|^2}{(\rho_n^{1/2} + \rho_m^{1/2})^2}, \tag{5}$$

where the $|\varphi_n\rangle$'s are the eigenvectors of $\rho = \sum_n \rho_n |\varphi_n\rangle\langle\varphi_n|$. In the following we will consider infinitesimally close states obtained upon varying a Hamiltonian parameter λ, and $\mathrm{d}\rho$ will correspond to $\mathrm{d}\rho = \partial\rho/\partial\lambda \mathrm{d}\lambda$. The above definition means that the bigger is the QCB distance, the smaller is the asymptotic error probability of discriminating a given states from its close neighbors.

In the following we will consider discrimination for ground and thermal states. In this case the eigenstates of ρ are those of the Hamiltonian and the distance may be written as the sum of two contributions

$$\mathrm{d}s^2_{\mathrm{QCB}} = \underbrace{\frac{1}{8}\sum_n \frac{(\mathrm{d}\rho_n)^2}{\rho_n}}_{\mathrm{d}s_c^2} + \underbrace{\frac{1}{2}\sum_{n\neq m} \frac{|\langle\varphi_n|\mathrm{d}\varphi_m\rangle|^2(\rho_n - \rho_m)}{(\rho_n^{1/2} + \rho_m^{1/2})^2}}_{\mathrm{d}s^2_{nc},}, \tag{6}$$

where $\mathrm{d}s_c^2$ refers to the classical part since it only depends on the Boltzmann weights of the eigenstates in the density operator, whereas $\mathrm{d}s^2_{nc}$ refers to the nonclassical one because it explicitly depends on the dependence of the eigenstates from the parameter of interest. If we consider the Ising model of the previous section and address discrimination of states labeled by different values of the coupling J, the QCB distance can be expressed by the metric g_J, $\mathrm{d}s^2_{\mathrm{QCB}} = g_J \mathrm{d}J^2$. We have [20]

$$g_J = \underbrace{\frac{\beta^2}{32}\sum_k \frac{(\partial_J \Lambda_k)^2}{\cosh^2(\beta\Lambda_k/2)}}_{g_J^c} + \underbrace{\frac{1}{4}\sum_k \tanh^2(\beta\Lambda_k/2)(\partial_J \vartheta_k)^2}_{g_J^{\mathrm{nc}}}. \tag{7}$$

Recent results about the Chernoff bound metric $\mathrm{d}s^2_{\mathrm{QCB}}$ [20,24] have shown that it may be used to investigate the phase diagram of the Ising model, i.e. to identify, in terms of different scaling with temperature, quasiclassical and quantum-critical regions. These results extend recent ones obtained using the Bures metric $\mathrm{d}s^2_{\mathrm{B}}$ (or the fidelity) [25–27], i.e.

$$\mathrm{d}s^2_{\mathrm{B}} = \frac{1}{2}\sum_{nm} \frac{\left|\langle\varphi_m|\,\mathrm{d}\rho|\varphi_n\rangle\right|^2}{\rho_n + \rho_m}. \tag{8}$$

In turn, one has the relation $\frac{1}{2}\mathrm{d}s^2_{\mathrm{B}} \le \mathrm{d}s^2_{\mathrm{QCB}} \le \mathrm{d}s^2_{\mathrm{B}}$ which shows that the Bures and the QCB metric have the same divergent behavior, i.e. one metric diverges if, and only if, the other does. Then one can exploit the results on the scaling behavior of the Bures metric derived in [25] to discriminate quantum states. Moreover, in the following we will see that when the system is in its ground state, $\mathrm{d}s^2_{\mathrm{QCB}} = \mathrm{d}s^2_{\mathrm{B}}$, whereas at increasing temperature T, $\mathrm{d}s^2_{\mathrm{QCB}} \to \frac{1}{2}\mathrm{d}s^2_{\mathrm{B}}$.

4. Discrimination of ground states

At zero temperature the system is in the ground state and the problem is that of discriminating two pure states corresponding to two different values J_1 and J_2 of the coupling J. The probability of error is given in terms of the overlap $|\langle\psi_1|\psi_2\rangle|^2$, whereas the minimum of $\mathrm{Tr}\left[\rho_1^s \rho_2^{1-s}\right]$ reduces to the overlap itself since for pure states $\rho^s = \rho \ \forall s$. Thus, the probability of error for the discrimination with n copies scales as $P_{e,n} \sim |\langle\psi_1|\psi_2\rangle|^{2n}$. In other words, the QCB may be expressed as $\xi_{\mathrm{QCB}} = -\log[4\ P_e(1 - P_e)]$. In this section we address the discrimination problem at zero temperature by evaluating the probability of error and the QCB metric, pointing out scaling properties, and minimizing (maximizing) them as a function of the external field. We first consider systems made of a few spins and then address the thermodynamic limit.

4.1. Short Ising chains, L = 2, 3, 4

The probability of making a misidentification P_e may be minimized by varying the value of the external field. For the case $L = 2$, 3 and 4, P_e is obtained by explicit

diagonalization of the Ising Hamiltonian. Minima of P_e correspond to the field value $\tilde{h} = (J_1 J_2)^{1/2}$, i.e. the geometrical mean of the two (pseudo) critical values, and follows the scaling behavior $P_{e,min}(J_1, J_2, (J_1 J_2)^{1/2}) = P_{e,min}(1, J_2/J_1, (J_2/J_1)^{1/2})$. More generally the probability of error is such that

$$P_e(kJ_1, kJ_2, kh) = P_e(J_1, J_2, h) \quad \forall k > 0. \tag{9}$$

Upon exploiting this scaling and fixing $J_1 = 1$ we can study P_e at $\tilde{h}$ as a function of $J_2 \equiv J$. The behavior of $Q(J) \equiv P_{e,min}(1, J, J^{1/2})$ is illustrated in Figure 1(*a*). The function has a cusp in $J = 1$, whereas the tails of the curve for $J \to 0$ and $J \to \infty$ go to zero faster with increasing size. This means that as the number of spins increases, the overlap between two different ground states approaches to zero. According to the scaling in Equation (9) the relevant parameter is the ratio between the two couplings and not the absolute difference. In turn, this means that $Q(J)$ is symmetric around $J = 1$ in a log-linear plot. Expanding $Q(J)$ around $J = 1$ and $J = 0$ we obtain the following behavior

$$\begin{aligned} Q(J) &\overset{J\simeq 1}{=} \frac{1}{2} - \alpha_L |J-1| + O|J-1|^2, \\ Q(J) &\overset{J\to 0}{=} \frac{1}{2} - A_L + \beta_L \sqrt{J} + \gamma_L J + O(J^{3/2}), \end{aligned} \tag{10}$$

where $\alpha_L \in (0, 1/2)$ is an increasing function of L. According to the scaling (9) the behavior of $Q(J)$ for large J is obtained by the replacement of $J \to 1/J$ in the second line of Equation (10). The parameters A_L, α_L, β_L, and γ_L are reported in Table 1 for $L = 2, 3, 4$. The corresponding Chernoff bound $\xi_J = -\log[4\,Q(J)\,(1 - Q(J))]$ does not carry additional information about the discrimination problem, but exhibits a simpler behavior

$$\begin{aligned} \xi_J &\overset{J\simeq 1}{=} \frac{\delta_L}{16} |J-1|^2 + O|J-1|^3, \\ \xi_J &\overset{J\to 0}{=} L \log 2 - L\sqrt{J} + \frac{L}{2} J + O(J^{3/2}), \end{aligned} \tag{11}$$

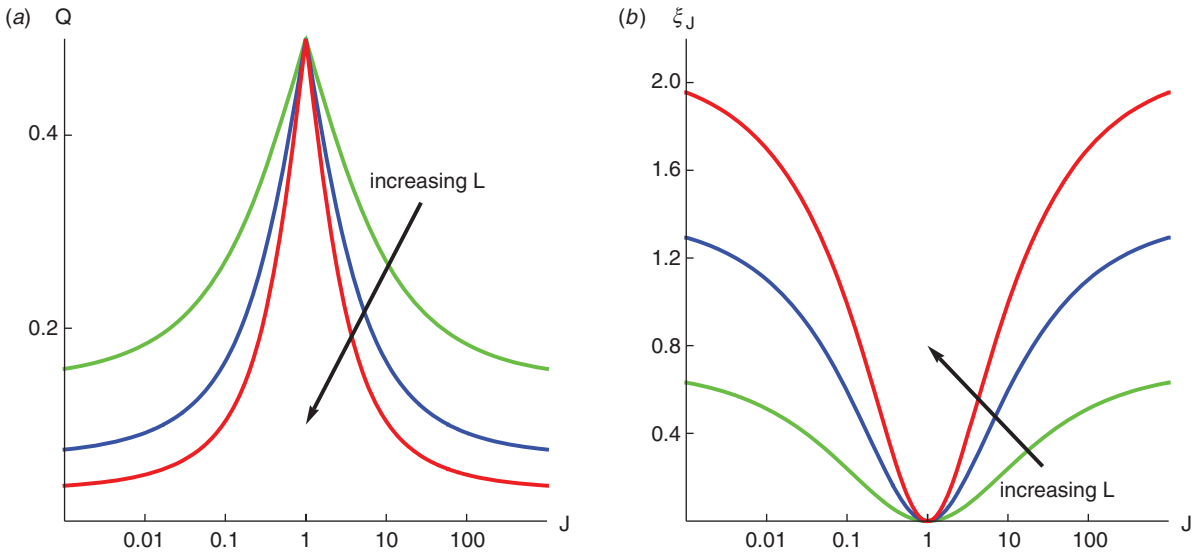

Figure 1. (*a*) Log-linear plot of the zero temperature rescaled minimum probability of error $Q(J) \equiv P_{e,min}(1, J, J^{1/2})$ as a function of J for $L = 2, 3, 4$ (green, blue and red lines, respectively). The function has a cusp in $J = 1$ and the two tails go to zero faster with increasing size. According to the scaling in Equation (9) the relevant parameter is the ratio between the two couplings and not the absolute difference. In the log-linear plot, this means that $Q(J)$ is symmetric around $J = 1$. (*b*) The Chernoff bound under the same conditions. (The color version of this figure is included in the online version of the journal.)

Table 1. Parameters. A_L, α_L, β_L, and γ_L appearing in Equation (10), i.e. the expansion of the rescaled probability of error $Q(J)$ around $J = 0$ and $J = 1$.

L	α	β	γ	A
2	$\alpha_2 = 1/8 = 0.125$	$\beta_2 = 1/2(2^{1/2}) \simeq 0.354$	$\gamma_2 = 1/4(2^{1/2}) \simeq 0.177$	$A_2 = 1/2(2^{1/2}) \simeq 0.354$
3	$\alpha_3 = 3^{1/2}/8 \simeq 0.217$	$\beta_3 = 3^{1/2}/8 \simeq 0.217$	$\gamma_3 = 5(3^{1/2})/32 \simeq 0.271$	$A_3 = 3^{1/2}/4 \simeq 0.433$
4	$\alpha_4 \simeq 0.306$	$\beta_4 = 1/2(14^{1/2}) \simeq 0.134$	$\gamma_4 = 23/28\ (14^{1/2}) \simeq 0.220$	$A_4 = 14^{1/2}/8 \simeq 0.468$

where $\delta_L = L!/4L$ for $L = 3$, 4 and half of this value for $L = 2$. The behavior of ξ_J for large J is again obtained by replacing $J \to 1/J$ in the second line of Equation (11). In Figure 1(*b*) we show ξ_J as a function of J for $L = 2, 3, 4$.

As mentioned in the previous section, when we compare ground states of Hamiltonians with infinitesimally close values of the coupling J, the proper measure to be considered is the QCB metric, with the point of maximal discriminability of two states corresponding to maxima of the QCB metric tensor. At zero temperature $\mathrm{d}s^2_{\mathrm{QCB}} = \mathrm{d}s^2_{\mathrm{B}}$ and thus [19]

$$\begin{aligned} g_J &= \frac{h^2}{4(h^2+J^2)^2}, \quad L = 2, \\ g_J &= \frac{3h^2}{16(h^2-hJ+J^2)^2}, \quad L = 3, \\ g_J &= \frac{h^2(h^4+4h^2J^2+J^4)}{4(h^4+J^4)^2}, \quad L = 4. \end{aligned} \tag{12}$$

Notice the simple scaling $g_J(kJ, kh) = g_J(J, h)$, which is valid $\forall L$. Maxima of g_J are thus obtained for $h^* = J$ for $L = 2, 3, 4$, and actually this is true for any L (see also the next section). The pseudo-critical point h^* which maximizes the QCB metric, turns out to be independent of L and equal to the true critical point, $h_c = J$, $\forall L$. At its maximum g_J goes like $1/J^2$ which means that it is easier to discriminate two infinitesimally close ground states for small J rather than for large ones.

4.2. Large L

For large L, the overlap (fidelity F) between two different ground states $|\psi_k\rangle \equiv |\psi_0(J_k)\rangle$, $k = 1, 2$ is given by

$$F = \langle \psi_1 | \psi_2 \rangle = \prod_k \cos \frac{\theta_{1k} - \theta_{2k}}{2}, \tag{13}$$

where $k = (2n+1)\pi/L$ and n runs from 1 to $L/2$. Obviously, $F = 1$ if $J_1 = J_2$. Otherwise, one has $\cos[(\theta_{1k} - \theta_{2k})/2] < 1$ and the fidelity F quickly decays as the ratio of the couplings is different from one. Solving $\partial_h \cos[(\theta_{1k} - \theta_{2k})/2] = 0$ one finds that the overlap has a cusp in $h = \pm(J_1 J_2)^{1/2}$, where it achieves the minimum value, corresponding to the minimum of the probability of error P_{e}. In the thermodynamic limit $L \to \infty$, the overlap between two different ground states goes to zero no matter how small is the difference in the parameters J_1 and J_2. In other words, the different ground states become mutually orthogonal, a behavior known as orthogonality catastrophe [28]. In the critical region, corresponding to the vanishing of one of the single particle energies $\epsilon_k^2 + \Delta_k^2 = 0$ with $k = 2\pi/L$, this behavior is enhanced, occurs for smaller L, and corresponds to a drop in the fidelity even for small values of $|J_2 - J_1|$.

For that which concerns the QCB metric, upon taking the limit $T \to 0$ in Equation (7), we have that the classical part $\mathrm{d}s_c^2$, which depends only on thermal fluctuations, vanishes due to the factor of $(\cosh(\beta\Lambda_k/2))^{-2}$. Therefore, at zero temperature only the nonclassical part of Equation (7) survives and one obtains $g_J = \frac{1}{4}\sum_k (\partial_J \vartheta_k)^2$, where

$$\partial_J \vartheta_k = \frac{1}{1 + (\Delta_k/\epsilon_k)^2} \left(\partial_J \frac{\Delta_k}{\epsilon_k} \right) = \frac{-h \sin k}{\Lambda_k^2}.$$

Since we are in the ground state, the allowed quasi-momenta are $k = [(2n+1)\pi]/L$ with $n = 0, \ldots, L/2 - 1$. Explicitly we have

$$g_J = \frac{1}{4} \sum_k \frac{h^2 \sin(k)^2}{\Lambda_k^4}. \tag{14}$$

We are interested in the behavior of the QCB metric in the quasi-critical region, which is described by small values of the scaling variable $z \equiv L(h - J) \simeq L/\xi$, that is $z \approx 0$. Conversely the off-critical region is given by $z \to \infty$. We substitute $h = J + z/L$ in Equation (14) and expand around $z = 0$ to obtain the scaling of g_J in the quasi-critical regime

$$\begin{aligned} g_J &= \frac{1}{4} \sum_{k_n} \frac{[J + (z/L)]^2 \sin^2(k_n)}{\left[(z^2/L^2) + 4J[J + (z/L)] \sin^2(k_n/2) \right]^2} \\ &\equiv \sum_{k_n} f_{k_n}(z). \end{aligned}$$

Since $\partial_z f(0) = 0$, the maximum of g_J is always at $z = 0$ for all values of L, in turn, the pseudo-critical point is $h^* = J = h_{\mathrm{c}}$ $\forall L$. Going to second order and using the Euler–Maclaurin formula, we get

$$g_J = \frac{L^2}{4} \left(\frac{1}{8J^2} - \frac{z^2}{384J^4} \right) - \frac{L}{8J^2} + O(L^0), \tag{15}$$

which shows explicitly that at $h = J$ the QCB metric has a maximum and there it behaves as

$$g_J \simeq \frac{L^2}{32J^2} + O(L). \tag{16}$$

From Equation (16) one concludes that the $1/J^2$ scaling of the metric may be compensated by using long chains, which thus appears as the natural setting to address the discrimination problem for large J.

5. Discrimination of thermal states

In this section we address the problem of discriminating two states at finite temperature, i.e. we consider two thermal states of the form $\rho_J = Z^{-1}\exp[-\beta H(J)]$,

$Z = \mathrm{Tr}\{\exp[-\beta H(J)]\}$, and analyze the behavior of the error probability, the Chernoff bound and the Chernoff metric as a function of the temperature and the external field. We discuss short chains $L = 2$, 3, 4 and then the case of large L.

5.1. *Short Ising chains L = 2, 3, 4*

For short chains we have evaluated the probability of error by explicit diagonalization of $\rho_2 - \rho_1$, with $\rho_k \equiv \rho_{J_k}$. The probability of error follows the scaling

$$P_e(kJ_1, kJ_2, kh, \beta/k) = P_e(J_1, J_2, h, \beta), \qquad (17)$$

which may be exploited to analyze its behavior upon fixing $J_1 = 1$. The main difference with the zero temperature case is that the error probability does depend on the absolute difference between the two couplings, and not only on the ratio between them. The optimal field $\tilde{h}$, minimizing $Q_\beta(J) = P_e(1, J, \tilde{h}, \beta)$ is zero for small J, then we have a transient behavior and finally, for large J, $\tilde{h} = J^{1/2}$. The range of J for which $\tilde{h} \simeq 0$ increases with temperature (small β). In Figure 2(*a*) we compare $Q_\beta(J)$ for $L = 2$ and different values of β to the analogous zero temperature quantity $Q_\infty(J)$. As is apparent from the plot the main effect of temperature is the loss of symmetry around $J = 1$. Analogous behavior may be observed for larger L. Notice that discrimination at finite temperature is not necessarily degraded.

Upon diagonalization of the Hamiltonian we have also evaluated the quantum Chernoff bound by numerical minimization of $\min_s \mathrm{Tr}\left[\rho_1^s \rho_2^{1-s}\right]$ and obtained for ξ_{QCB} the same scaling properties (17) observed for the error probability. In Figure 2(*b*) we compare the QCB for $L = 2$ and different values of β to the analogous zero temperature quantity. Again the main effect of temperature is the loss of symmetry around $J = 1$. Analogous behavior may be observed for larger L. For vanishing J the Chernoff bound $\xi_{\mathrm{QCB}}(1, J \to 0, J^{1/2}, \beta) \equiv \xi_0$ saturates to a limiting value scaling with β as

$$\xi_0 \simeq \beta^2/2, \quad \beta \to 0, \qquad (18)$$

$$\xi_0 \simeq \frac{\sqrt{2}}{\pi} \arctan(\beta/2), \quad \beta \to \infty. \qquad (19)$$

On the other hand, for diverging J, $\xi_{\mathrm{QCB}}(1, J \to \infty, J^{1/2}, \beta) \equiv \xi_\infty$ shows the non-monotone behaviour illustrated in Figure 3(*b*). In Figure 3(*a*) we report ξ_0 as a function of β together with the approximating functions of Equations (18) and (19). Overall, we notice that both for the single-copy and many-copy case, increasing the temperature may also result in an improvement of discrimination, at least in the region of large couplings and intermediate temperatures.

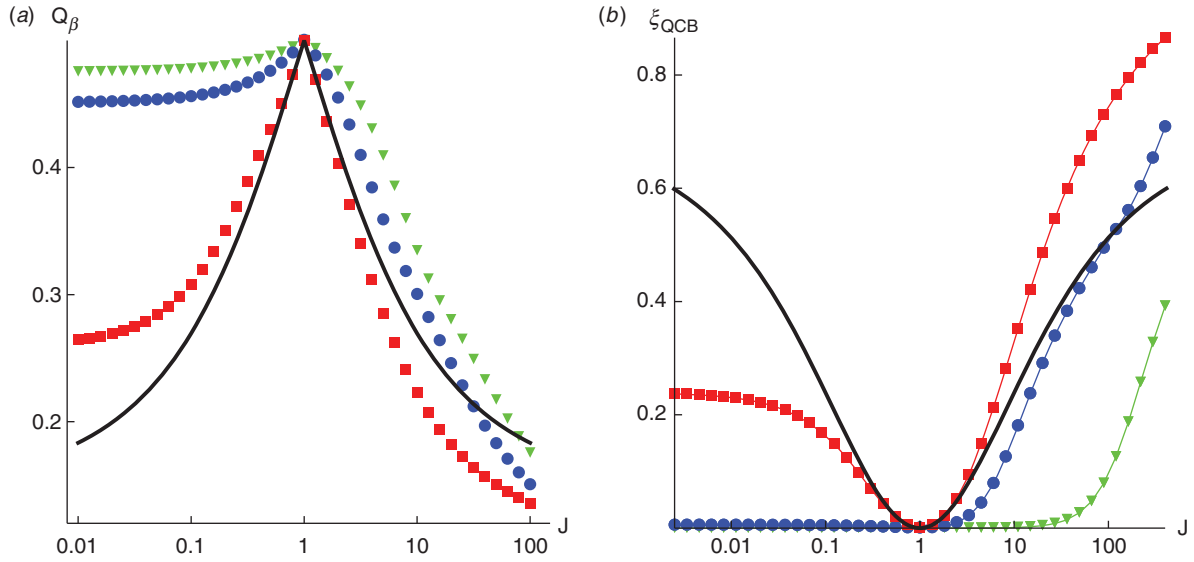

Figure 2. (*a*) Log-linear plot of the rescaled minimum probability of error $Q_\beta(J) \equiv P_{e,\min}(1, J, J^{1/2}, \beta)$ for $L = 2$ as a function of J. Green triangles correspond to $\beta = 0.05$, blue circles to $\beta = 0.1$ and red squares to $\beta = 1$. The black solid curve is the probability of error in the zero temperature case. The main effect of temperature is the loss of symmetry around $J = 1$. (*b*) Log-linear plot of the quantum Chernoff bound ξ_{QCB} for $L = 2$. Green triangles correspond to $\beta = 0.05$, blue circles to $\beta = 0.1$ and red squares to $\beta = 1$. We also report the zero temperature QCB for comparison (solid black curve). (The color version of this figure is included in the online version of the journal.)

Finally, we have evaluated the QCB metric and found that it follows the scaling

$$g_J(J,h,\beta) = \beta^2 \Phi_L(\beta J, \beta h), \tag{20}$$

where the form of the function Φ_L depends on the size only. The same scaling is also true for the Bures metric with different functions Φ_L. Indeed, this behavior follows directly from the common structure of the two metrics and by the fact that g_J is obtained from the square of the derivative with respect to J. The scaling is actually true for any size L. The optimal value h^* of the external field, which maximizes the QCB metric at fixed J and β may be found numerically. Upon exploiting the scaling properties we consider $\beta = 1$ and found that h^* is zero for small J, then we have a transient behavior and finally, for large J, $h^* = J$. According to the scaling above, the range of J for which $h^* \simeq 0$ increases with temperature (small β) and vice versa. In turn, for $\beta \to \infty$ we recover the results of the previous section, i.e. the critical point is always the optimal one for discrimination. This behavior is illustrated in Figure 4(*a*), where we report the optimal field h^* as a function of J for $\beta = 1$. The inset shows the small J region. As we have noticed in the previous section the two metrics are equal in the zero temperature limit. For finite temperature this is no longer true and a question arises on whether the whole range of values allowed by the inequality $ds^2_B/2 \leq ds^2_{QCB} \leq ds^2_B$

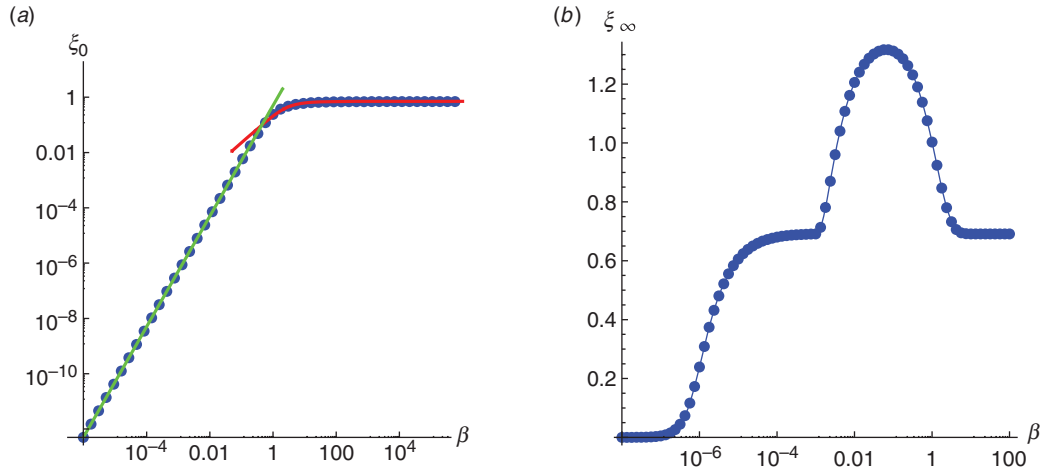

Figure 3. (*a*) Log-log plot of the Chernoff bound for vanishing J, $\xi_0 \equiv \xi_{QCB}(1, J \to 0, J^{1/2}, \beta)$, as a function of inverse temperature β (blue points) together with the approximating functions of Equation (18) (green line) and (19) (red line). (*b*) Log-linear plot of the Chernoff bound for diverging J, $\xi_\infty \equiv \xi_{QCB}(1, J \to \infty, J^{1/2}, \beta)$, as a function of inverse temperature β. (The color version of this figure is included in the online version of the journal.)

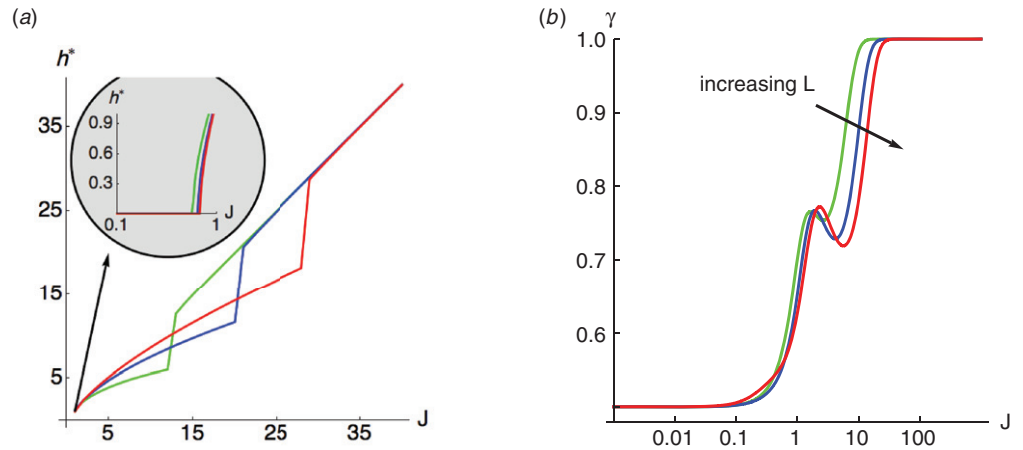

Figure 4. (*a*) Linear plot of the optimal field h^* maximizing the QCB metric as a function of J for $\beta = 1$. The inset shows the region of small J. (*b*) Log-linear plot of the ratio γ between the (maximized) QCB and Bures metrics as a function of J for $L = 2$, 3, 4 (green, blue and red lines, respectively) and $\beta = 1$. (The color version of this figure is included in the online version of the journal.)

is actually spanned by the QCB metric. This is indeed the case, as may be seen by analyzing the behavior of the ratio $\gamma = \mathrm{d}s^2_{\mathrm{QCB}}/\mathrm{d}^2_{\mathrm{B}}s$ at the (pseudo) critical point h^* (we take the maximum of both the metrics, which generally occurs at different values of the field). In Figure 4(*b*) we report γ as a function of J for $\beta = 1$ and $L = 2, 3, 4$. As it is apparent from the plot, for small J we have $\mathrm{d}s^2_{\mathrm{QCB}} \simeq \frac{1}{2}\mathrm{d}s^2_{\mathrm{B}}$, whereas for large J the two quantities become equal $\mathrm{d}s^2_{\mathrm{QCB}} \simeq \mathrm{d}s^2_{\mathrm{B}}$. The ratio is not monotone and the dependence on the size is weak. Upon exploiting the scaling in Equation (20) we may easily see that the range of J for which the two metrics are almost equal increases with β. For vanishing temperature ($\beta \to \infty$) $\mathrm{d}s^2_{\mathrm{QCB}} \simeq \mathrm{d}s^2_{\mathrm{B}}$ everywhere and we recover the results of the previous section. Conversely, for high temperature we have $\mathrm{d}s^2_{\mathrm{QCB}} \simeq \frac{1}{2}\mathrm{d}s^2_{\mathrm{B}}$ also for very large J. Also the transient region is shrinking for increasing temperature.

5.2. Large L

In the limit of large size L the behavior of the Chernoff metric follows the same scaling of Equation (20) found for short chains. The optimal value of the field which maximizes the QCB metric is $h^* = J$ for any finite temperature, where the metric element has a cusp. We have studied the QCB metric in the quantum-critical region $\beta|J-h| \ll 1$ and for low temperature $T \to 0$. The classical elements of the metric vanish due to the factor $1/\cosh^2(\beta\Lambda_k/2)$ and we are left to analyze the nonclassical part g^{nc}_J as a function of T. Bounding the metric by functions that have the same scaling behavior in β [20], will ensure that the metric itself scales with the same exponent. The dispersion relation is linear around $k = 0$ and we approximate $\Lambda_k \sim Jk$ at the critical point $J = h$. Upon defining

$$f(\beta,k) = \begin{cases} \beta^2k^2/4, & 0 \le k \le 2/\beta, \\ 1, & 2/\beta \le k \le \pi, \end{cases}$$

we have, for all β and k, $\frac{1}{2}f(\beta,k) < \tanh^2(\beta Jk/2) < f(\beta,k)$. For large L, the sum on the classical part of the QCB metric may be replaced by the integral $L\int \mathrm{d}k$, thus leading to

$$g^{\mathrm{nc}}_J \simeq \frac{L}{2\pi}\int_0^{2/\beta} \mathrm{d}k \tanh^2(\beta Jk/2)\frac{1}{J^2k^2} + \frac{L}{2\pi}\int_{2/\beta}^{\pi} \mathrm{d}k \tanh^2(\beta\Lambda_k/2)\frac{J^2\sin^2(k)}{\Lambda_k^4}. \quad (21)$$

This is a good approximation in the limit $\beta \to \infty$ because the upper integration limit $2/\beta$ becomes arbitrarily close to 0. The first integral is bounded by

$$\frac{L}{2\pi}\int_0^{2/\beta} \mathrm{d}k \frac{f(\beta,k)}{2}\frac{1}{J^2k^2} \le \frac{L}{2\pi}\int_0^{2/\beta} \mathrm{d}k \tanh^2(\beta Jk/2)\frac{1}{J^2k^2} \le \frac{L}{2\pi}\int_0^{2/\beta} \mathrm{d}k f(\beta,k)\frac{1}{J^2k^2}.$$

The bounding integrals scale as $L\beta$ and the first integral must scale in the same way for $\beta \to \infty$. The second term is upper bounded by

$$\frac{L}{2\pi}\int_{2/\beta}^{\pi} \mathrm{d}k \tanh^2(\beta\Lambda_k/2)\frac{J^2\sin^2(k)}{\Lambda_k^4} \le \frac{L}{2\pi}\int_{2/\beta}^{\pi} \mathrm{d}k \frac{1}{J^2k^2} \sim L\beta.$$

Therefore, since the bounding integral scales as βL, g^{nc}_J must scale as βL to the highest order. Observe that in the quantum-critical region $g_J \sim L$ is extensive, whereas at the critical point it has a superextensive behavior $g_J \sim L^2$. The nonclassical element scales algebraically with temperature and in the zero temperature limit it diverges, matching the ground state behavior that we described in the previous section. These results remark that criticality provide a resource for quantum state discrimination, and that the discrimination of quantum states is indeed improved upon approaching the QCP.

6. Conclusions

We have addressed the problem of discriminating two ground states or two thermal states corresponding to different values of the coupling constant in the one-dimensional quantum Ising model. We have analyzed both short and long chains with the aim of assessing the role of criticality (pseudo criticality for short chains) in single-copy and many-copy discrimination as well as in the discrimination of infinitesimally closed states.

At zero temperature both, the error probability for single-copy discrimination, and the Chernoff bound for n-copy discrimination in the asymptotic limit, are optimized by choosing the external field as the geometric mean of the two (pseudo) critical points. In this regime, the relevant parameter governing both quantities is the ratio between the two values of the coupling constant. On the other hand, the Chernoff metric is equal to the Bures metric and is maximized at the (pseudo) critical point. For finite temperature we have analyzed in some detail the scaling properties of all the above quantities and have derived the optimal external field. We found that the effect of finite temperature is twofold. On the one hand, critical values of the field are optimal only for large values of the coupling constants. On the other hand, the ratio between the couplings is no longer the only relevant parameter for both the error probability and the

Chernoff bound, which also depends on the absolute difference. The ratio between the Chernoff metric and the Bures metric decreases continuously, but not monotonically, for increasing temperature and approaches 1/2 in the limit of high-temperature.

In conclusion, upon considering the one-dimensional Ising model as a paradigmatic example we have quantitatively shown how and to which extent criticality may represent a resource for state discrimination in many-body systems.

Acknowledgements

The authors thank Paolo Giorda, Lorenzo Campos Venuti, Marco Genoni, Paolo Zanardi, and Michael Korbman for stimulating discussions.

References

[1] Helstrom, C.W. *Quantum Detection and Estimation Theory;* Academic Press: New York, 1976.
[2] Chefles, A. *Contemp. Phys.* **2000,** *41,* 401–424.
[3] Bergou, J.A.; Herzog, U.; Hillery, M. Discrimination of Quantum States. In *Quantum State Estimation*: Rehacek, J., Paris, M.G.A., Eds.; Lecture Notes in Physics 649; Springer: Berlin, 2004; pp 417–465.
[4] Chefles, A. Quantum States: Discrimination and Classical Information Transmission. A Review of Experimental Progress. In *Quantum State Estimation*: Rehacek, J., Paris, M.G.A., Eds.; Lecture Notes in Physics 649; Springer: Berlin, 2004; pp. 467–511.
[5] Ivanovic, I.D. *Phys. Lett. A* **1987,** *123,* 257–259.
[6] Dieks, D. *Phys. Lett. A* **1988,** *126,* 303–306.
[7] Peres, A. *Phys. Lett. A* **1988,** *128,* 19.
[8] Jaeger, G.; Shimony, A. *Phys. Lett. A* **1995,** *197,* 83–87.
[9] Ban, M. *Phys. Lett. A* **1996,** *213,* 235–238.
[10] Kennedy, R.S. *MIT Res. Lab. Electron. Quart. Progr. Rep.* **1973,** *110,* 142–146.
[11] Ban, M.; Kurokawa, K.; Momose, R.; Hirota, O. *Int. J. Theor. Phys.* **1997,** *36,* 1269–1288.
[12] Eldar, Y.C.; Megretski, A.; Verghese, G.C. *IEEE Trans. Inform. Theory* **2003,** *IT-49,* 1007–1012.
[13] Chou, C.-L.; Hsu, L.Y. *Phys. Rev. A* **2003,** *68,* 042305, [quant-ph/03044117].
[14] Barnett, S.M. *Phys. Rev. A* **2001,** *64,* 030303(R).
[15] Andersson, E.; Barnett, S.M.; Gilson, C.B.; Hunter, K. *Phys. Rev. A* **2002,** *65,* 052308.
[16] Audenaert, K.M.R.; Calsamiglia, J.; Munoz-Tapia, R.; Bagan, E.; Masanes, L.; Acin, A.; Verstraete, F. *Phys. Rev. Lett.* **2007,** *98,* 160501.
[17] Calsamiglia, J.; Munoz-Tapia, R.; Masanes, L.; Acin, A.; Bagan, E. *Phys. Rev. A* **2008,** *77,* 032311.
[18] Zanardi, P.; Paris, M.G.A.; Campos Venuti, L. *Phys. Rev. A* **2008,** *78,* 042105.
[19] Invernizzi, C.; Korbman, M.; Campos Venuti, L.; Paris, M.G.A. *Phys. Rev. A* **2008,** *78,* 042106.
[20] Abasto, D.F.; Jacobson, N.T.; Zanardi, P. *Phys. Rev. A* **2008,** *77,* 022327.
[21] Osborne, T.J.; Nielsen, M.A. *Phys. Rev. A* **2002,** *66,* 032110.
[22] Osterloh, A.; Amico, L.; Falci, G.; Fazio, R. *Nature (London)* **2002,** *416,* 608–610.
[23] Vidal, G.; Latorre, J.I.; Rico, E.; Kitaev, A. *Phys. Rev. Lett.* **2003,** *90,* 227902.
[24] Bauer, B.; Scarola, V.W.; Troyer, M.; Whaley, K.B. Distinguishing Phases with Ansatz Wavefunctions. 2009, arXiv:0903.1454 e-Print archive. http://lanl.arxiv.org/pdf/0903.1454 (accessed Mar 8, 2009).
[25] Zanardi, P.; Campos Venuti, L.; Giorda, P. *Phys. Rev. A* **2007,** *76,* 062318.
[26] Zhou, H.Q.; Orus, R.; Vidal, G. *Phys. Rev. Lett.* **2008,** *100,* 080601.
[27] Zhou, H.Q.; Barjaktarevic, J.P. Fidelity and Quantum Phase Transitions. 2007, arXiv: cond-mat/0701608 e-Print archive. http://lanl.arxiv.org/abs/cond-mat/0701608 (accessed Jan 25, 2007); Zhou, H.Q.; Zhao, J.H.; Li, B. Fidelity Approach to Quantum Phase Transition: Finite Size Scaling for Quantum Ising Model in a Transverse Field. 2007, arXiv:0704.2940 e-Print archive. http://lanl.arxiv.org/pdf/0704.2940 (accessed Apr 23, 2007).
[28] Zanardi, P.; Paunković, N. *Phys. Rev. E* **2006,** *74,* 031123.